Tutorial

Rob Bates*

The modern miniature camera objective: an evolutionary design path from the landscape lens

Abstract: The modern miniature camera lens is the most prolific design manufactured today, yet its design form and origins are often not well understood. This paper illuminates the ancestry of the modern miniature camera lens by developing the lens form from 'scratch.' Starting with the Wollaston meniscus of 1812, the lens is designed progressively, employing incremental design decisions aimed at correcting limiting aberrations at each step. The result demonstrates an ancestry that is distinctly different than that of the common large-format objective lenses.

Keywords: aspheric surfaces; camera objective; mobile phone cameras; optical design; polymer.

OCIS codes: 220.0220; 220.1000; 220.3620; 220.1250; 160.5470; 000.2850.

***Corresponding author: Rob Bates,** FiveFocal LLC, 1600 Range Street, Boulder, CO 80301, USA, e-mail: rob.bates@fivefocal.com

1 Introduction

The history of the camera objective, as chronicled by Kingslake in 1989, is a fascinating look at the evolution of lens design in response to burgeoning optical materials, advances in manufacturing processes, and changes in design specifications [1]. Since the completion of that work, the rise of digital imaging and postprocessing capabilities have changed the modern camera and led to an expansion of lens design to system-level design, often identified as 'computational imaging.' These advances have resulted in unusual new designs, but the large-format digital cameras that are in popular use still have objective lenses that draw on an unmistakable ancestry illuminated by Kingslake's work.

The camera objective in the compact camera module does not draw on the same ancestry as the common large-format lens employed in digital imaging. Compared to a large-format lens, the miniature camera objective meets and overcomes a different set of challenges, as described by a recent paper by Steinich and Blahnik [2]. Owing to the demand for compact track length, exploitation of optical grade polymers, and advances in injection molding, the result is a lens form that appears very different from the large-format lens. Figure 1 demonstrates a recent sample from the patent literature that is indicative of the form [3].

Contrasted to a typical large-format camera objective, like any of the double Gauss derivatives, there appears to be an evolutionary jump in the history of lens design leading to the unusual-looking modern miniature camera objective. However, this is not strictly the case; the double Gauss does not provide the correct standard for comparison. Many modern patents from Olympus and Konica Minolta describe a four-element miniature camera objective as an inverted Ernostar [4, 5]. When viewed from that perspective, the miniature camera objective does not appear as unusual with its very forward aperture stop positioning, asymmetric design, and power placement.

This tutorial seeks to build the family tree of the modern miniature camera objective by designing the lens from 'scratch,' following closely the development of forms identified in Kingslake's original work. We will identify its ancestry along the way and demonstrate that the lens design form of the most widely used camera objective in history can be found through a logical progression of design choices starting from the first camera objective.

2 Design specifications and considerations

The compact camera module specifications that have been the driving force for change are a reduced track length and low cost, a motivation clearly captured in early designs that were still rather traditional in form [6]. As with Kodak's attempts to minimize the cost in the 1950s with the Dakon line of lenses, the volume production of plastic elements became an attractive solution for cost. Following this material choice, the highly aspheric, thin element shapes enabled by injection molded plastic elements provided an additional leverage to reduce the track length.

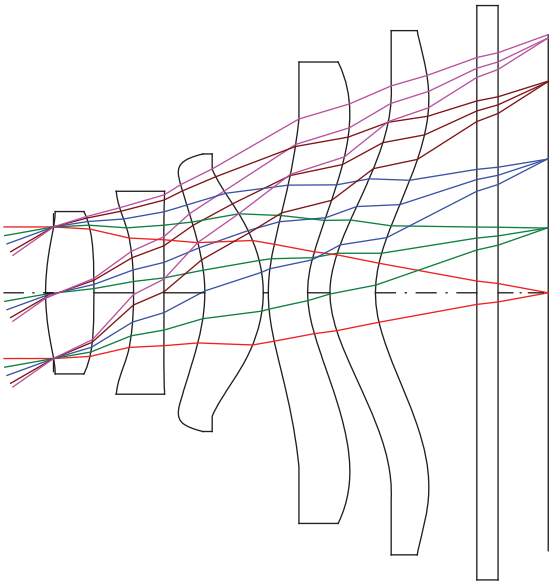

Figure 1 Modern f/2.8 five-plastic element miniature camera objective with 80° full field of view and 3.63 mm effective focal length from 2012 U.S. Patent 8,189,273. The telephoto ratio is 1.35.

While cost and track length forced the change, a demand for a higher performance, faster lenses supporting larger-format imagers have accelerated the evolution of the miniature camera objective. In 2007, the first-generation iPhone was released with an f/2.8 camera objective paired with a 2-MP array. Now in 2012, the f/2.4 camera objective is a five-element lens paired with an 8-MP array, and the camera module is claimed to be 25% shorter than it was a year ago. For this tutorial, the lens will be designed to specifications that are similar to the current iPhone lens with precision injection molding as the manufacturing method. These specifications and design constraints are provided in Table 1.

As the following lens design will begin with poorly performing origins, the design performance will first be described in terms of RMS spot diameter, and the lenses will be designed to operate at an f/# with a target maximum of 14 μm RMS spot diameter over the field, as this tends to produce f-numbers similar to the original use. Only in the final stage will the performance be reported using the more relevant MTF performance metric.

Table 1 Miniature camera objective specifications.

Parameter	Value
Effective Focal Length (EFL)	4.1 mm
f/#	2.4
Sensor array	3264×2448
Pixel pitch	1.4 μm
Sensor format	Bayer pattern, backside illumination
Maximum chief ray angle	30°, nonlinear
|Distortion|	<2%
Relative illumination	>50%
Element center and thickness	>0.30 mm
Total Track Length (TTL)	<4.5 mm
Back Focal Length (BFL)	>1 mm (accommodates IR-cut filter and cover glass)
Element surface slopes	<45°

3 Progressive design of modern camera objective

3.1 Starting point: landscape lens of 1812

The first photographic objective that achieved a larger FOV at 60° full field was provided by Wollaston in 1812, nearly 25 years before photography was invented [7]. It took the form of a meniscus element separated from the aperture stop and operated at f/15.

We begin with this starting point by scaling the system to the 4.1-mm Effective Focal Length (EFL). We also shift immediately to plastic in place of glass, as we will be targeting a plastic-only solution. As one of the limiting aberrations in this design is lateral chromatic aberration, this influences the selection. For this single element lens with the stop fixed in the 'natural,' coma-free location, the lateral color can only be reduced by increasing the Abbe number. Thus, PMMA is selected as it represents a plastic crown.

An implementation of this solution with a flat tangential field is demonstrated in Figure 2. The spot diagram in Figure 2 shows that the flat tangential field balances two of the limiting aberrations of this lens – the sagittal spread of the spot due to the sagittal field curvature against the tangential spread of the spot due to the lateral color.

Along with the sagittal field curvature and lateral chromatic aberration, there are other limiting aberrations in this lens. The third is the 5% barrel distortion. The fourth is unseen here because the system has been stopped down to f/14 to maintain a 14-μm RMS spot diameter. As the aperture is increased, the spherical aberration will quickly overwhelm the other aberrations. In total, this is a difficult starting point for the goals in Table 1.

3.2 Reducing track length with reversed meniscus

There are several directions one could take from the landscape lens starting point, and we choose to work on the track length first. This is useful at this early stage to gain an understanding of the limits of space as the design progresses.

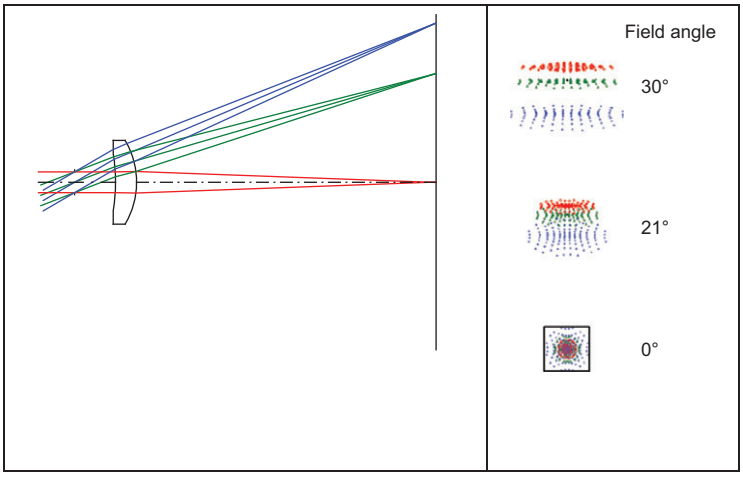

Figure 2 Wollaston meniscus lens with a flat tangential field. The spot diagram at the right demonstrates the trade between lateral color and sagittal field curvature. Scale is provided by the square surrounding the on-axis ray bundle, which is 10 μm on each side.

Track length will be reduced easily by changing to the alternate form of the landscape lens with the stop behind the lens. This lens, shown in Figure 3, has a Total Track Length (TTL) of 3.84 mm compared to the 5.15 mm before.

The reversed landscape lens is a compromise of performance for form, as was understood by those at Kodak who marketed the solution in 1934. Compared to the specifications in Table 1, the track length requirement is now met, but the performance is degraded. The lens must be stopped down to f/22 to maintain an RMS spot diameter of 14 μm. The lens also suffers from a pincushion distortion of 8.5%.

3.3 Reducing odd aberrations through symmetry

At this point, one could choose to achromatize the lens, but with the available plastics, a new achromat is not possible, and the old achromat will shorten the already troublesome Petzval radius. In fact, such a design will decrease the Petzval radius from -2.1 to -1.4 times the focal length. Instead, we choose to follow the path that G. S. Cundell took in 1844 and apply symmetry to the design. The symmetry about the stop will correct the odd aberrations, of which lateral color and distortion are two of the limiting aberrations of the current lens. This design is shown in Figure 4.

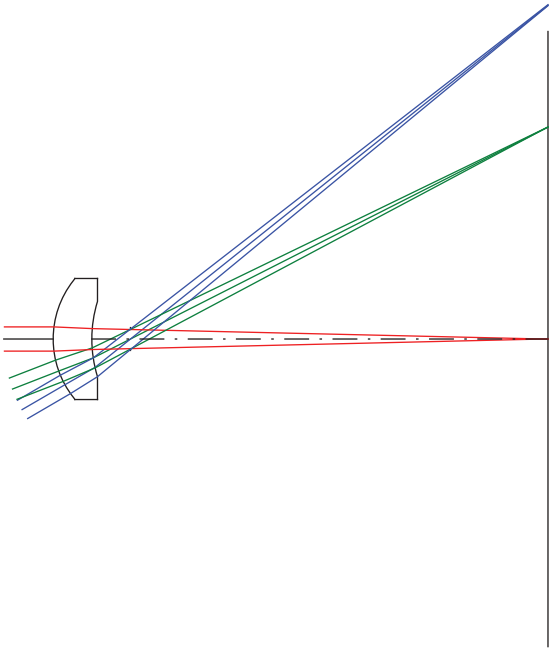

Figure 3 Reversed meniscus lens with a flat tangential field operating at f/22 with a reduced track length at 3.84 mm.

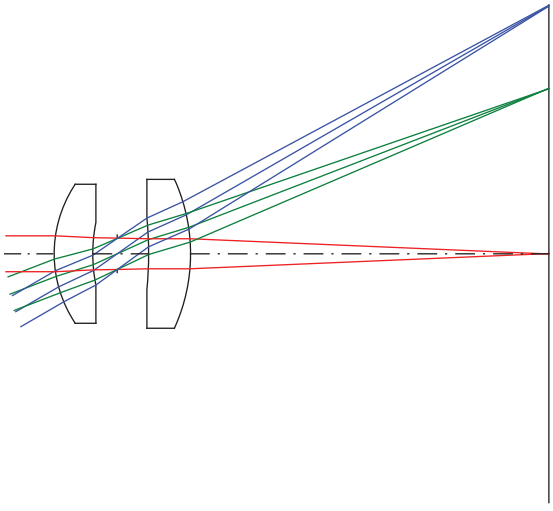

Figure 4 Symmetric meniscus lenses positioned about the stop reduce the odd aberrations. The lens is f/12.

This step in the design process has virtually eliminated two of the limiting aberrations, with lateral chromatic aberration nearly zero and distortion at -0.4%. The system is now operating at f/12 to maintain an extreme field RMS spot diameter less than 14 μm. However, increasing the numerical aperture further would extend the track length, which is already increasing beyond 4.7 mm.

In addition to spherical aberration, the field curvature is now one of the limiting aberrations in this system. The Petzval radius has decreased to -1.6f, which is better than the achromatic solution, but worse than the reversed landscape lens. In an attempt to correct this problem, further optimization will tend to form the second lens into a high, positive shape factor with a large displacement from the stop, significantly increasing the ray angles at this lens. Another way to reduce the Petzval sum is to increase the index of the second lens by changing it to PEI, but this greatly degrades the distortion for little field curvature improvement. As the performance of this lens is decent, we are going to leave the correction of the field curvature for a while and address the issue of increasing the numerical aperture of this solution.

3.4 Increasing the numerical aperture with an achromatic doublet

As one considers Figure 4 with plastic lenses in mind, there is little hesitation to apply a fourth order asphere to the second surface of the first element to correct spherical aberration as the speed of the lens increases. As we are looking to develop the lens through a more traditional path, and our last step was in 1844, we will, instead, apply an achromatic doublet at this point to help both the spherical aberration and axial color.

Although a cemented doublet is not generally used in high volume plastic lenses, we will begin with such an element knowing we will break the cemented interface later. We replace the first element of the symmetric meniscus design with an achromat, retaining PMMA as the positive element and adding to it a negative SAN element. Alternative achromats exist, but this provides a good balance of spherical aberration and distortion, while the design is driven to f/6. The result, shown in Figure 5 with its ray aberration curve, is similar to the Aldis lens of 1901 [8].

At this point, the f/6 lens has a maximum RMS spot diameter of 14 μm. The lens is 4.5 mm long, and the distortion is -3%. The field is strongly curved, with a Petzval radius of -1.5f.

3.5 Increasing the numerical aperture and improving performance with a triplet

In order to improve the spherical aberration correction and gain some greater control over the design variables, the cemented doublet was broken, and the lens takes on the form of Dennis Taylor's Cooke triplet from 1893. This design is shown in Figure 6 along with its ray fan. When compared to the ray fan of the Aldis lens, it is clear that there is a significant similarity in performance, with the broken cement interface enabling better spherical and color correction. Not indicated by the ray fan is the greatly improved distortion, which is now only 0.4% at its maximum.

At this point, we optimize the materials, driving the inner flint to the high index, high dispersion PEI. With this material set, the Cooke triplet form can be further pushed to a speed of f/4.5 with a maximum RMS spot diameter of 14 μm and a 4.5-mm track length. In doing so, the distortion increases a little to 1.4%.

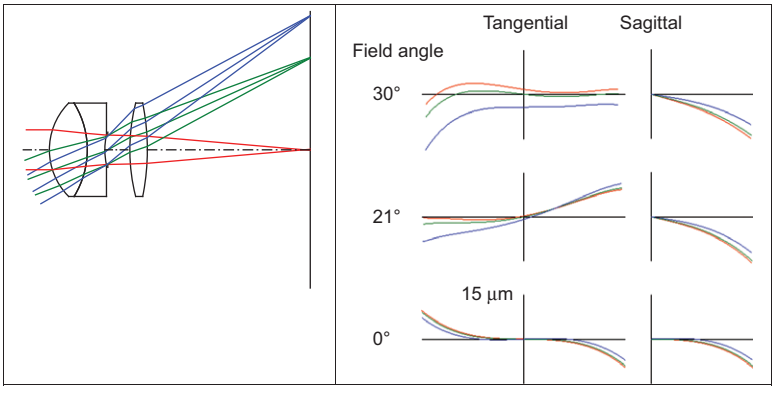

Figure 5 Lens form similar to that of Aldis from 1901. The achromatic doublet enables the lens to operate at f/6. Ray fan at the right is shown with blue, green, and red colors for wavelengths corresponding to the F, d, and C Fraunhofer lines, respectively.

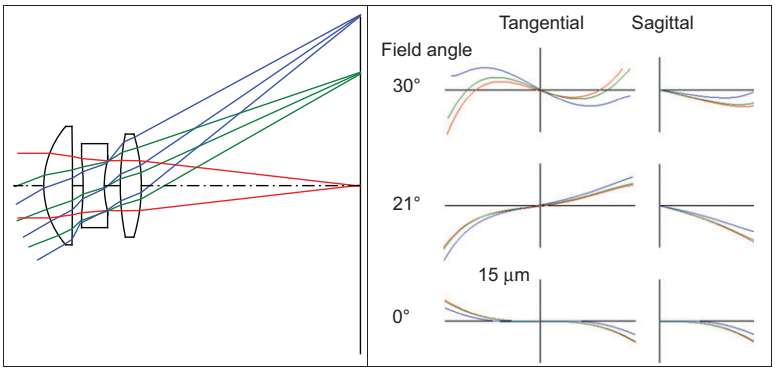

Figure 6 Cooke triplet from 1893, operating at f/4.5. The ray fan at the right is shown with blue, green, and red colors for wavelengths corresponding to the F, d, and C Fraunhofer lines, respectively.

3.6 Flattening the field

The paths forward from this position are numerous. One option is to move to a split triplet, though the typical split of the front element is not attractive because of the length restriction. We could also choose to add a thick meniscus to the back of the lens. This improves the Petzval radius from -1.8f to -2.8f and is also a nicely balanced solution, enabling the lens to be pushed to f/3.2 before reaching an RMS spot diameter of 13 µm. Taking this path would lead to a similar end form, but the transitions are not as graceful.

Instead, we will give up a little performance and choose to focus on the Petzval radius by adding a negative field flattener and moving the stop forward. In doing so, we are priming the lens to be in a better position to achieve the chief ray angle constraint, and the Petzval radius can be greatly improved to -4.6f. The resulting design shown in Figure 7 is very similar to the objective patented by Imai in 1981, as well as the lens used for the Kodak Disc camera in 1982 [9].

The lens is now operating at f/3.4 with a maximum RMS spot diameter of 13 µm. The distortion is 2%, and the total track length is 4.5 mm.

3.7 Adding aspheric surfaces to increase the numerical aperture

At this point, the limiting aberration is still spherical aberration if the f/# is to be driven toward f/2.4. To mitigate this problem, we add a single fourth-order asphere to the back of the first element, just as Kodak did with their plastic first element. The resulting lens is easily pushed to f/2.4, though the field performance drops off at the edge. An aspheric last element (also in line with the original lens form) enables us to improve that condition and at last meet the chief ray angle requirements of Table 1, as well as most of the other requirements. The lens could be pushed to a shorter length on par with its focal length, but we will keep the 4.5-mm track length in order to retain room for an additional lens. This lens is shown in Figure 8.

The lenses in Figures 7 and 8 are difficult to classify. Warren Smith calls this form ‘unusual’ and regards it as a member of the wide-angle family with one negative outer element, a telephoto, or a triplet with a field corrector [10]. Both Kingslake and Imai refer to this form as a wide-angle telephoto. At its core, the lens is similar to an inversion of Minor’s 1916 invention known first as the Ultrastigmat, a general form more famously known as an Ernostar [11]. There are some examples found in the patent literature between 1940 and 1960 that are, to some degree, similar to the solution shown in Figure 9

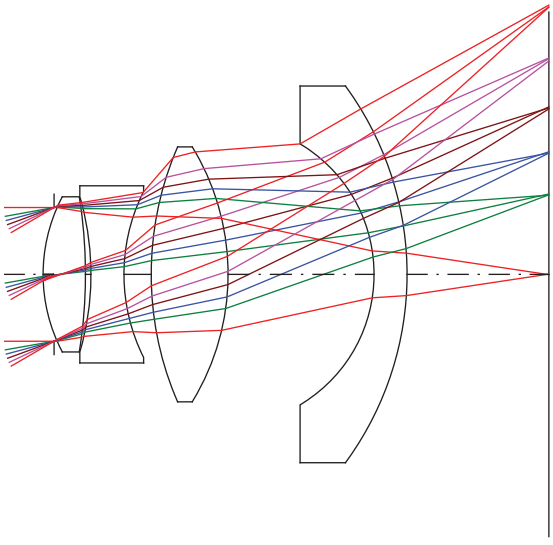

Figure 7 F/3.4 triplet with a field flattener and forward located stop improves the Petzval radius.

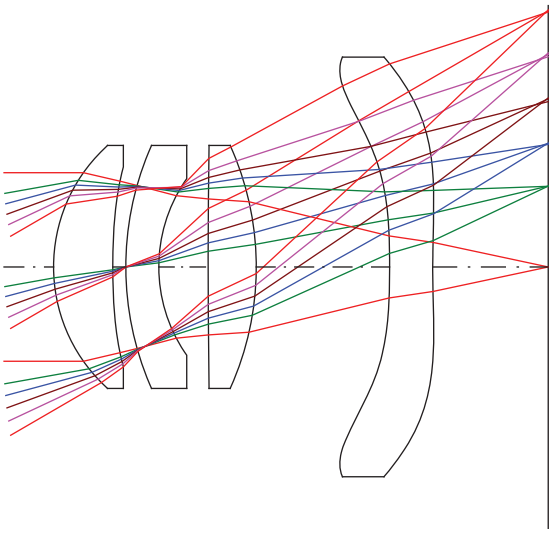

Figure 8 Inverted Ernostar objective operating at f/2.4. The second surface of the first element has a fourth-order asphere, and the last element is described by the fourth- and sixth-order aspheres on both surfaces.

and its variants, but too superficial to claim a more direct relationship [12–15].

The lens is now f/2.4 with a maximum RMS spot diameter of 14 µm. The track length is 4.5 mm, and the chief ray angle constraint, as well as the surface slope constraints, is met. The distortion ranges from -2% to 2%.

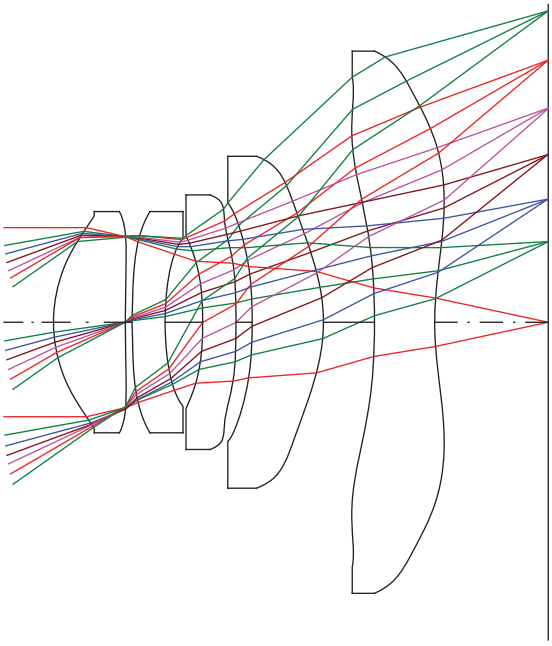

Figure 9 The final f/2.4 five-plastic element design meeting the specifications with a 4.1-mm effective focal length and 70° full field of view. All surfaces are aspheric of varying order, up to the 14th order. The telephoto ratio is 1.1.

3.8 Optimizing to the final design form

At last, the design is ready to take on its final form. We increase the field, split the third element, and aspherize all surfaces to improve the performance. This design is shown in Figure 9.

The design meets the specifications from Table 1 with a 4.1-mm EFL, 70° full field of view, 4.5 mm track length, and 1 mm back focal length, which allows room for focus, an IR cut filter, and sensor cover glass. All edge and center thickness constraints are met, and element surface slopes are minimized. The chief ray angles are less than 30° at the sensor, and the relative illumination at the edge of the field is 59%. As shown in Figure 10, the distortion ranges from -2% to 2%.

For the performance, it is more relevant at this point to present an MTF metric. The MTF shown in Figure 11 demonstrates that the lens has been optimized for good nominal performance. A nearby solution designed for high

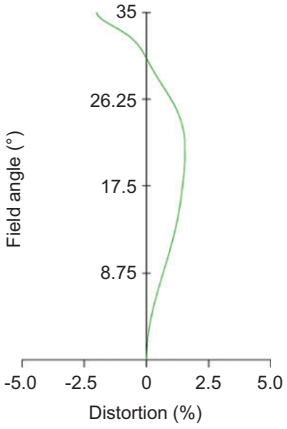

Figure 10 Distortion plot for five-plastic element miniature camera objective.

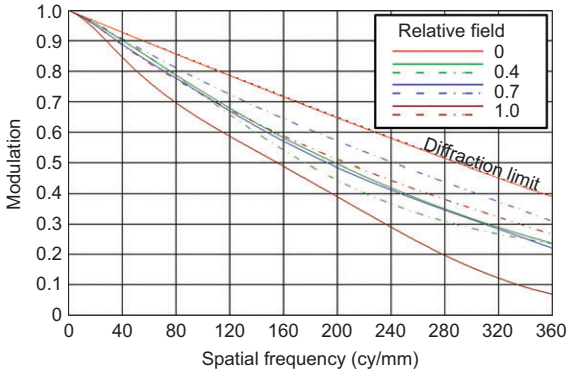

Figure 11 MTF for five-plastic element miniature camera objective. The fields are defined by their relative heights out to the 35° field angle. The tangential MTF is indicated by solid lines, the sagittal MTF is indicated by dashed lines.

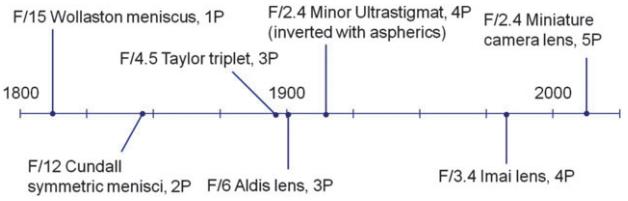

Figure 12 The modern miniature camera lens progressive design timeline. F-numbers are attributed according to the resultant design in this study and do not necessarily correlate to the original use. The number of plastic elements is indicated after the lens name.

yield would have been optimized to trade little nominal performance in order to make the solution as robust to manufacturing errors as possible, as demonstrated previously by the author [16].

4 Conclusions

The modern, miniature camera objective can be developed using incremental steps between forms created over the last 200 years of lens design, producing a time line as shown in Figure 12.

In developing the form of the modern miniature camera objective, we started with the Wollaston meniscus lens of 1812 and reduced the length of the lens by reversing its placement with the aperture stop. Odd aberrations were corrected through the introduction of a second lens, which provided symmetry about the aperture stop, in the fashion of Cundell. Spherical aberration was improved through the introduction of a doublet, enabling the system to take on a higher numerical aperture in the form of Aldis lens. The achromatic doublet was split to achieve the Taylor triplet and allow a better control over all Seidel aberrations to reduce the f/# further. A field flattener was added to improve the Petzval radius, resulting in a solution similar to Imai's. Aspheric surfaces enabled independent correction of spherical aberration as well as a better control of the field curves and distortion while meeting the constraints of the chief ray angle of incidence at the sensor. This culminated in meeting the goal of f/2.4 operation with a lens similar to an inversion of Minor's Ultrastigmat. The final lens performance was optimized while meeting the design constraints through the introduction of aspheric surfaces throughout.

The design process demonstrates how a lens of presumably unusual design may be conceived and also gives rise to a kind of family tree. In this development, we find that the modern miniature camera lens extends from the Cooke triplet on a different path than that of the common large-format objective. The large-format objective lens follows from the triplet along the lines of the split triplet, Ernostar, Sonnar, Tessar, and double Gauss forms. Owing to its space constraints, the miniature camera objective follows from the triplet as a compact wide-angle telephoto that is most closely related to an inverted Ernostar from 1916 or Imai's patent from 1979.

Received November 13, 2012; accepted December 13, 2012

References

[1] R. Kingslake, 'A History of the Photographic Lens' (Academic Press, London, 1989).
[2] T. Steinich and V. Blahnik, Adv. Opt. Techn. 1, 51–58 (2012).
[3] S. Noda, 'Imaging Lens Assembly', U.S. Patent 8,189,273 B2 (2012).
[4] Y. Kamo, 'Image formation optical system and imaging system incorporating the same', U.S. Patent 7,206,143 B2 (2007).
[5] M. Sato, 'Image pickup lens, image pickup apparatus, and mobile terminal provided with image pickup apparatus', U.S. Patent 7,215,492 B2 (2007).
[6] H. Yamada, 'Imaging lens', U.S. Patent 5,940,219 (1999).
[7] W. H. Wollaston. Phil. Mag. 41, 124 (1813).
[8] H. Aldis, 'Photographic lens', U.S. Patent 682,017 (1901).
[9] T. Imai, 'Photographic lens system', U.S. Patent 4,303,313 (1981).
[10] W. Smith, 'Modern Lens Design' (McGraw-Hill, U.S., 2005).
[11] C. Minor, 'Photographic objective', U.S. Patent 1,360,667 (1920).
[12] F. Altman, 'Lens', U.S. Patent 2,343,629 (1942).
[13] W. Orser, 'Optical scanning objective lens system for inspection devices', U.S. Patent 2,747,466 (1956).
[14] I. Sandback, 'Optical objective', U.S. Patent 3,011,401 (1961).
[15] W. Johnson, 'Optical objective', U.S. Patent 3,011,402 (1961).
[16] R. Bates, Proc. SPIE 7793, 779302 (2010). Available at http://proceedings.spiedigitallibrary.org/proceeding.aspx?articleid=1347508.

Rob Bates received his M.S. in Optical Science from the University of Arizona in 2008 with an emphasis on lens design desensitization to manufacturing errors. He began his optical engineering career over a decade earlier, first specializing in scientific instrument optical system design in 1997. After moving to Colorado to join Ball Aerospace in 2002, he designed space telescope systems and supported the optical analysis of the James Webb Space Telescope until 2006. From 2006 to 2009, he was an optical engineer at CDM Optics where he became deeply involved in the design for the manufacture of high-volume miniature camera lenses and computational imaging systems. Since 2009, he has been the Director of Optical Engineering at FiveFocal LLC, developing advanced imaging systems from visible through LWIR with consumer, defense, and biomedical applications. In 2010, he provided the top solution to the International Optical Design Competition, building the solution 'from scratch' as demonstrated in this paper.